Photosynth Res (2017) 132:211–220
DOI 10.1007/s11120-017-0340-8

TECHNICAL COMMUNICATION

Simple generalisation of a mesophyll resistance model for various intracellular arrangements of chloroplasts and mitochondria in C_3 leaves

Xinyou Yin[1] · **Paul C. Struik**[1]

Received: 8 July 2016 / Accepted: 17 January 2017 / Published online: 14 February 2017

Abstract The classical definition of mesophyll conductance (g_m) represents an apparent parameter ($g_{m,app}$) as it places (photo)respired CO_2 at the same compartment where the carboxylation by Rubisco takes place. Recently, Tholen and co-workers developed a framework, in which g_m better describes a physical diffusional parameter ($g_{m,dif}$). They partitioned mesophyll resistance ($r_{m,dif} = 1/g_{m,dif}$) into two components, cell wall and plasmalemma resistance (r_{wp}) and chloroplast resistance (r_{ch}), and showed that $g_{m,app}$ is sensitive to the ratio of photorespiratory (F) and respiratory (R_d) CO_2 release to net CO_2 uptake (A): $g_{m,app} = g_{m,dif}/[1+\omega(F+R_d)/A]$, where ω is the fraction of r_{ch} in $r_{m,dif}$. We herein extend the framework further by considering various scenarios for the intracellular arrangement of chloroplasts and mitochondria. We show that the formula of Tholen et al. implies either that mitochondria, where (photo)respired CO_2 is released, locate between the plasmalemma and the chloroplast continuum or that CO_2 in the cytosol is completely mixed. However, the model of Tholen et al. is still valid if ω is replaced by $\omega(1-\sigma)$, where σ is the fraction of (photo)respired CO_2 that experiences r_{ch} (in addition to r_{wp} and stomatal resistance) if this CO_2 is to escape from being refixed. Therefore, responses of $g_{m,app}$ to $(F+R_d)/A$ lie somewhere between no sensitivity in the classical method ($\sigma=1$) and high sensitivity in the model of Tholen et al. ($\sigma=0$).

✉ Xinyou Yin
Xinyou.yin@wur.nl

[1] Centre for Crop Systems Analysis, Wageningen University & Research, P.O. Box 430, 6700 AK Wageningen, The Netherlands

Keywords CO_2 transfer · Internal conductance · Mesophyll resistance

Introduction

The biochemical C_3 photosynthesis model of Farquhar, von Caemmerer and Berry (1980), the FvCB model hereafter, has been widely used to interpret leaf physiology from gas exchange measurements. The model calculates the net rate of leaf photosynthesis (A) as the minimum of the Rubisco carboxylation activity-limited rate (A_c) and the electron (e^-) transport-limited rate (A_j) of photosynthesis (see Appendix A). The partial pressure of CO_2 at the carboxylation sites of Rubisco in the chloroplast stroma (C_c) is a required input variable to calculate both A_c and A_j in the model. The drawdown of C_c, relative to the CO_2 level in the ambient air (C_a), depends not only on stomatal conductance for CO_2 transfer (g_{sc}), but also on the mesophyll conductance for CO_2 transfer between substomatal cavities and the site of CO_2 carboxylation (g_m). According to Fick's diffusion law, g_m can be expressed as follows (von Caemmerer and Evans 1991; von Caemmerer et al. 1994):

$$g_m = A/(C_i - C_c) \quad (1)$$

where C_i is the partial pressure of CO_2 at the intercellular air spaces.

This simple gas diffusion equation has been combined with the FvCB model to estimate g_m (Pons et al. 2009), based on combined data of A–C_i curves and chlorophyll fluorescence measurements on photosystem II e^- transport efficiency Φ_2 (Harley et al. 1992; Yin and Struik 2009) or on combined gas exchange and carbon isotope discrimination measurements (Evans et al. 1986). When the g_m estimation is based on combined gas exchange and chlorophyll

fluorescence measurements (e.g. the 'variable J method', Harley et al. 1992), the A_j part of the FvCB model is used, in which the linear e^- transport rate (J) is estimated from chlorophyll fluorescence signals. Using this method, it has been reported that g_m can decrease with increasing C_i or with decreasing incoming irradiance I_{inc} (Flexas et al. 2007; Vrábl et al. 2009; Yin et al. 2009). Similar patterns of variable g_m have been reported with the isotope discrimination method (Vrábl et al. 2009), although with less consistency (Tazoe et al. 2009).

Equation (1) is based on net photosynthesis and assumes that respiratory and photorespiratory CO_2 release occurs in the same compartment as CO_2 fixation by Rubisco. However, CO_2 fixation occurs in the chloroplast stroma, whereas (photo)respiratory CO_2 is released in the mitochondria. The first step of photorespiration, the O_2 fixation, takes place in the chloroplast to form phosphoglycolate. Phosphoglycolate is converted to glycolate and glyoxylate, and then to glycine in the peroxisome; glycine moves to the mitochondria and is decarboxylated there into CO_2, NH_3 and serine (Kebeish et al. 2007). The CO_2 released in mitochondria, from either respiration or photorespiration, can be partially refixed by Rubisco in the chloroplast stroma, whereas the remaining portion escapes to the atmosphere (Busch et al. 2013). To quantify mesophyll resistance r_m (the reciprocal of g_m), there is a need to specify resistance components within the cell imposed by walls, plasmalemma, cytosol, chloroplast envelope and stroma (Evans et al. 2009; Terashima et al. 2011). Unlike the CO_2 that comes from the substomatal cavities, the CO_2 from the mitochondria does not need to cross the cell wall and plasmalemma, and thus experiences a different resistance. Considering this difference, Tholen et al. (2012) developed a theoretical framework to analyse g_m as described below.

The total mesophyll diffusional resistance ($r_{m,dif}$) can be described as the sum of a series of physical resistances comprising of intercellular air space, cell wall, plasmalemma, cytosol, chloroplast envelope and chloroplast stroma components (Evans et al. 2009): $r_{m,dif} = r_{ias} + r_{wall} + r_{plasmalemma} + r_{cytosol} + r_{envelope} + r_{stroma}$. The resistance imposed by the gas phase component and the cytosol is generally small (Tholen et al. 2012), and may therefore be ignored. Tholen et al. (2012) combined r_{wall} and $r_{plasmalemma}$ into the resistance at the cell wall–plasma membrane interface (r_{wp}), and $r_{envelope}$ and r_{stroma} into the total chloroplast resistance (r_{ch}), so that $r_{m,dif} = r_{wp} + r_{ch}$. Based on Fick's diffusion law and considering two different resistance components encountered by CO_2 from substomatal cavities and CO_2 from the mitochondria, Tholen et al. (2012) derived the following relationship (their Eq. 6):

$$C_c = C_i - A\left(r_{wp} + r_{ch}\right) - (F + R_d)r_{ch} \quad (2)$$

where F is the photorespiratory CO_2 release and R_d is the CO_2 release in the light other than by photorespiration, both in the mitochondria. The model Eq. (2) is still a simplification of true resistance pathways, because (i) diffusion is a continuous process and there are many parallel pathways (Tholen et al. 2012) and (ii) the model ignores that some respiratory flux originates in the chloroplast (Tcherkez et al. 2012) and that there may be small activity of phospho*enol*pyruvate carboxylase in cytosol (Douthe et al. 2012; Tholen et al. 2012).

Here we let $r_{ch} = \omega r_{m,dif}$; then $r_{wp} = (1-\omega)r_{m,dif}$, where ω is the relative contribution of r_{ch} to the total mesophyll resistance $r_{m,dif}$ ($= r_{wp} + r_{ch}$). Equation (2) then becomes

$$C_c = C_i - Ar_{m,dif} - \omega(F + R_d)r_{m,dif} \quad (3)$$

Solving ($C_i - C_c$) from Eq. (3) and substituting it into Eq. (1) give

$$g_m = \frac{1}{r_{m,dif}\left(1 + \omega\frac{F+R_d}{A}\right)} \quad (4)$$

Equation (4) is equivalent to Eq. (9) of Tholen et al. (2012), in which g_{wp} and g_{ch} (i.e. the inverse of r_{wp} and r_{ch}, respectively) are used. We prefer Eq. (4) because it allows (i) to analyse how g_m varies for a given total mesophyll resistance and (ii) to provide an analogue to an extended model that will be developed later.

Both Eq. (4) and Tholen et al.'s Eq. (9) tell that g_m, as defined by Eq. (1), is influenced by the ratio of (photo) respiratory CO_2 from the mitochondria to net CO_2 uptake $(F + R_d)/A$, thereby resulting in an apparent sensitivity of g_m to CO_2 and O_2 levels (Tholen et al. 2012). This sensitivity does not imply a change in the intrinsic diffusion properties of the mesophyll; so, g_m as defined by Eqs. (1) and (4) is apparent, and we denote it as $g_{m,app}$ hereafter. The sensitivity depends on ω: the higher is ω the more sensitive is $g_{m,app}$ to $(F + R_d)/A$. If $\omega = 0$, then $g_{m,app}$ is no longer sensitive to $(F + R_d)/A$, Eq. (3) becomes Eq. (1) and $g_{m,app}$ becomes $g_{m,dif}$—the intrinsic mesophyll diffusion conductance ($= 1/r_{m,dif}$). In such a case, carboxylation and (photo) respiratory CO_2 release occur in the same organelle compartment or if occurring in separate compartments, the chloroplast exerts a negligible resistance to CO_2 transfer.

Equations (1) and (2) have been considered as two basic scenarios for CO_2 diffusion path in C_3 leaves (von Caemmerer 2013), both representing a simplified view on CO_2 diffusion in the framework of whole leaf resistance models. Detailed views on the mechanistic basis of CO_2 diffusion in relation to intracellular organelle positions could best be investigated using reaction–diffusion models (e.g. Tholen and Zhu 2011). However, uncertainties in the value of many required input diffusion coefficients and the complexity in nature are the major limitations of using these

reaction–diffusion models (see Berghuijs et al. 2016 for discussions on simple resistance vs. reaction–diffusion models). We herein discuss an extended, yet simple, resistance model by considering various scenarios with regard to intracellular arrangement of organelles: (1) the relative positions of mitochondria and chloroplasts and (2) gaps between individual chloroplasts. We also discuss implications of these scenarios in estimating the fraction of (photo) respired CO_2 being refixed.

A generalised model

To develop a generalised model, we consider two possibilities of chloroplast distribution (either continuous or discontinuous) and three possibilities of mitochondria location (outer, inner or both outer and inner layers of cytosol). This gives six cases with regard to the arrangement of organelles within mesophyll cells (Fig. 1). In each scenario, mitochondria are intimately associated with chloroplasts, as commonly observed for real leaves (Sage and Sage 2009; Hatakeyama and Ueno 2016). Within our simple generalised model, we stay with the same notation of r_{wp} and r_{ch}, the two-resistance components as the essence of the model of Tholen et al. (2012). However, as we discuss later on, instead of assuming that $r_{cytosol}$ is negligible, we followed the approach of Berghuijs et al. (2015) that lumps part of $r_{cytosol}$ into r_{wp} and the remaining part of $r_{cytosol}$ into r_{ch}. Given the position of mitochondria shown in Fig. 1, nearly all cytosolic resistance, i.e. along the diffusion path length from plasmalemma to chloroplast outer membrane, can be lumped into $r_{wp,}$ whereas only a small remaining portion of $r_{cytosol}$ is lumped into r_{ch}.

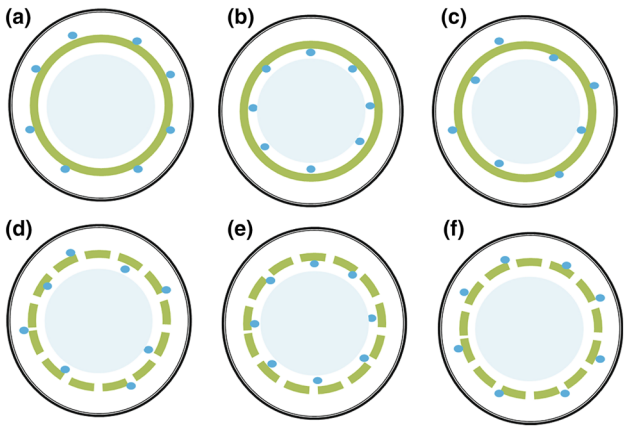

Fig. 1 Schematic illustration of six scenarios for the arrangement of organelles in the mesophyll cell. In each panel, the *outer double-lined black circle* indicates the combined cell wall and plasmalemma, the *green circle* indicates chloroplast continuum (panels a–c) or the *green circle* segments indicate chloroplasts (panels d–f), the filled small *blue symbols* indicate mitochondria and the *inner light blue circle* represents vacuole

Case I

In this case, the coverage of chloroplasts is continuous and all mitochondria locate in the outer layer of cytosol (Fig. 1a). For this case, the net CO_2 influx (A) from the intercellular air spaces is driven by the gradient between C_i and $C_{m(outer)}$ (where $C_{m(outer)}$ is the CO_2 partial pressure at the outer layer of the mesophyll cytosol facing chloroplast envelope), whereas the gradient between $C_{m(outer)}$ and C_c drives the carboxylation flux (V_c). Therefore, equations for the CO_2 gradient between the compartments and involved resistance components are as follows: $C_c = C_{m(outer)} - V_c r_{ch}$ and $C_{m(outer)} = C_i - A r_{wp}$. In the FvCB model, A is formulated as $A = V_c - F - R_d$. Combining these three equations actually gives rise to Eq. (2), from which Eq. (4) for the sensitivity of $g_{m,app}$ to $(F + R_d)/A$ was derived. Therefore, formulae for this Case I are in line with the framework as described by Tholen et al. (2012).

Tholen et al. (2012) also showed, based on their model framework, that the fraction of (photo)respired CO_2 that is refixed by Rubisco can be quantified using the resistance components. We use $x(F + R_d)$ to denote the partial pressure of (photo)respired CO_2 in mesophyll cytosol, where x is a conversion factor from flux to partial pressure for (photo)respired CO_2 and has a unit of bar (mol m^{-2} $s^{-1})^{-1}$. CO_2 molecules from (photo)respiration can diffuse towards Rubisco but will experience r_{ch} and a resistance derived from the carboxylation itself (r_{cx}); so the refixation rate (R_{refix}) is $x(F + R_d)/(r_{ch} + r_{cx})$. A portion of the (photo)respired CO_2 molecules can also escape from refixation and move out of the stomata to the atmosphere, experiencing r_{wp} and the stomatal resistance for CO_2 transfer r_{sc} (including a small boundary layer resistance); so the rate of this leak or escape (R_{escape}) is $x(F + R_d)/(r_{wp} + r_{sc})$. The fraction of (photo)respired CO_2 that is refixed by Rubisco (f_{refix}) can be calculated by

$$f_{refix} = \frac{R_{refix}}{R_{refix} + R_{escape}} = \frac{\frac{1}{r_{ch}+r_{cx}}}{\frac{1}{r_{ch}+r_{cx}} + \frac{1}{r_{wp}+r_{sc}}} = \frac{r_{sc} + r_{wp}}{r_{sc} + r_{wp} + r_{ch} + r_{cx}} \quad (5)$$

This compares with Eq. (14) of Tholen et al. (2012) and shows that the refixation fraction can be calculated simply as the ratio of the resistance components that the escaped (photo)respired CO_2 molecules have experienced to the total resistance along the full diffusion pathway.

Case II

The coverage of chloroplasts is continuous and all mitochondria locate in the inner layer of cytosol, closely behind chloroplasts (Fig. 1b). In this case, since there are no mitochondria between the plasmalemma and chloroplasts, in essence, r_{ch} and r_{wp} can be combined and the flux involved is the same for the CO_2 gradient between C_i and $C_{m(outer)}$ and between $C_{m(outer)}$ and C_c, i.e. A ($=V_c–F–R_d$). This corresponds to the classical model, Eq. (1), that has commonly been used for estimating g_m (von Caemmerer and Evans 1991; von Caemmerer et al. 1994).

In this case, all (photo)respired CO_2 molecules have to experience r_{ch}, in addition to r_{wp} and r_{sc}, if they are to escape from being refixed. As mitochondria locate closely behind chloroplasts and mitochondria and chloroplasts are treated essentially as one compartment in the classical model, (photo)respired CO_2 molecules that diffuse towards Rubisco can be considered to experience r_{cx} only; so R_{refix} is $x(F+R_d)/r_{cx}$. The remaining (photo)respired CO_2 that escape from refixation experience r_{ch}, r_{wp} and r_{sc}; so, R_{escape} is $x(F+R_d)/(r_{ch}+r_{wp}+r_{sc})$. Then, f_{refix} can be calculated by

$$f_{refix} = \frac{R_{refix}}{R_{refix}+R_{escape}} = \frac{\frac{1}{r_{cx}}}{\frac{1}{r_{cx}}+\frac{1}{r_{ch}+r_{wp}+r_{sc}}} = \frac{r_{sc}+r_{wp}+r_{ch}}{r_{sc}+r_{wp}+r_{ch}+r_{cx}} \quad (6)$$

Obviously, this predicts a higher refixation fraction than Eq. (5) does.

Case III

The coverage of chloroplasts is continuous and mitochondria locate in both inner and outer layers of cytosol (Fig. 1c). Let λ be the fraction of mitochondria that locate closely behind chloroplasts in the inner cytosol. Then $(1-\lambda)$ is the fraction of mitochondria that locate in the outer cytosol. The flux associated with the gradient between $C_{m(outer)}$ and C_c is the carboxylation flux (V_c) minus the efflux of (photo)respired CO_2 from the inner layer $\lambda(F+R_d)$, while the flux associated with the gradient between C_i and $C_{m(outer)}$ is still A. Therefore, equations for the CO_2 gradients between the compartments and involved resistance components are as follows:

$$C_c = C_{m(outer)} - [V_c - \lambda(F+R_d)]r_{ch} \quad (7)$$

$$C_{m(outer)} = C_i - Ar_{wp} \quad (8)$$

Equation (7) without R_d would be comparable to the third equation in Fig. 4 of von Caemmerer (2013) for modelling the photorespiratory bypass engineered by Kebeish et al. (2007). Combining Eqs. (7) and (8) with $V_c = A+F+R_d$ gives rise to an equation in analogy to Eq. (2):

$$C_c = C_i - A(r_{wp}+r_{ch}) - (1-\lambda)(F+R_d)r_{ch} \quad (9)$$

The same logic as for Eqs. (3) and (4) gives

$$g_{m,app} = \frac{1}{r_{m,dif}\left[1+\omega(1-\lambda)\frac{F+R_d}{A}\right]} \quad (10)$$

Equation (10) suggests that the apparent g_m as defined by Eq. (1) is still sensitive to $(F+R_d)/A$, although the sensitivity factor changes from ω for Case I to $\omega(1-\lambda)$ now for Case III.

For this case, either refixed or escaped (photo)respired CO_2 molecules have two parts, one part from the inner and the other from outer cytosol, and they experience different resistant components. Assuming for the purpose of simplicity that mitochondria are distributed in such a way that any variation in x between inner and outer cytosol is negligible, the refixed (photo)respired CO_2 molecules R_{refix} can easily be expressed as $\lambda x(F+R_d)/r_{cx} + (1-\lambda)x(F+R_d)/(r_{ch}+r_{cx})$, whereas the escaped (photo)respired $CO_2 R_{escape}$ can be expressed as $\lambda x(F+R_d)/(r_{ch}+r_{wp}+r_{sc}) + (1-\lambda)x(F+R_d)/(r_{wp}+r_{sc})$. Then, f_{refix} can be calculated by

$$f_{refix} = \frac{R_{refix}}{R_{refix}+R_{escape}} = \frac{\frac{\lambda}{r_{cx}}+\frac{1-\lambda}{r_{ch}+r_{cx}}}{\frac{\lambda}{r_{cx}}+\frac{1-\lambda}{r_{ch}+r_{cx}}+\frac{\lambda}{r_{ch}+r_{wp}+r_{sc}}+\frac{1-\lambda}{r_{wp}+r_{sc}}} \quad (11)$$

This expression for f_{refix} looks rather unwieldy but it covers Eqs. (5) and (6) for the previous two cases when λ is 0 and 1, respectively.

Case IV

This is the most general case, in which the coverage of chloroplasts is discontinuous and mitochondria locate in both inner and outer layers of cytosol (Fig. 1d). If chloroplast coverage is discontinuous, it is possible that some mitochondria lie exactly in the chloroplast gaps. This situation can be simplified by assigning part of (photo)respired CO_2 in the gaps to the inner and the other part to the outer cytosol; so, λ is still defined as for Case III as the fraction of mitochondria that locate in the inner cytosol. However, another factor needs to be introduced to account for the direct effect of the chloroplast gaps as these gaps allow the diffusion of (photo)respired CO_2 from the inner to the outer cytosol and vice versa. In our context here, we only need to define k as the factor allowing for a decrease ($0 \le k < 1$) or an increase ($k > 1$) in the fraction of inner (photo)respired CO_2, caused by the chloroplast gaps. Then, Eq. (7) can be simply adjusted for Case IV:

$$C_c = C_{m(outer)} - [V_c - k\lambda(F+R_d)]r_{ch} \quad (12)$$

while Eq. (8) remains unchanged. Then, equations for case IV, equivalent to Eqs. (9–11) for case III, can be easily defined by replacing the places of λ with $k\lambda$. This also

means that the fraction of outer (photo)respired CO_2 now becomes $(1-k\lambda)$.

In fact, the lumped $k\lambda$ can be re-defined as a single factor σ, which refers to the fraction of (photo)respired CO_2 molecules that have to experience r_{ch}, in addition to r_{wp} and r_{sc}, if they are to escape from being refixed. Then, a more general form of Eq. (3) or Eq. (9) becomes

$$C_c = C_i - Ar_{m,dif} - \omega(1-\sigma)(F+R_d)r_{m,dif} \quad (13)$$

and a more general form of Eqs. (10) and (11) becomes

$$g_{m,app} = \frac{1}{r_{m,dif}\left[1+\omega(1-\sigma)\frac{F+R_d}{A}\right]} \quad (14)$$

$$f_{refix} = \frac{R_{refix}}{R_{refix}+R_{escape}} = \frac{\frac{\sigma}{r_{cx}} + \frac{1-\sigma}{r_{ch}+r_{cx}}}{\frac{\sigma}{r_{cx}} + \frac{1-\sigma}{r_{ch}+r_{cx}} + \frac{\sigma}{r_{ch}+r_{wp}+r_{sc}} + \frac{1-\sigma}{r_{wp}+r_{sc}}} \quad (15)$$

As σ has a value between 0 and 1, it follows that the factor k varies between 0 and $1/\lambda$. This suggests that the lower the λ is, the more likely it is that $k>1$. However, the exact value of k and how k modifies λ (e.g. via the path between the chloroplasts vs through the chloroplast) are hard to quantify from the simple resistance model. As large gaps between chloroplasts decrease S_c/S_m, the ratio of chloroplast surface area to mesophyll surface area exposed to the intercellular air spaces (Sage and Sage 2009; Tholen et al. 2012; Tomas et al. 2013), the value of k must be associated with S_c/S_m. However, k may also depend on factors such as the CO_2 influx from the intercellular air spaces. These dependences of k on λ, S_c/S_m, and other factors could best be analysed using reaction–diffusion models like the one by Tholen and Zhu (2011).

Two more special cases

Now we consider two more special cases. The first instance is the case in which the coverage of chloroplasts is discontinuous and all mitochondria locate in the inner layer of cytosol (Fig. 1e), and the second is that the coverage of chloroplasts is discontinuous and all mitochondria locate in the outer layer of cytosol (Fig. 1f). The diffused amount of (photo)respired CO_2 from the inner to the outer cytosol (for the first instance) or from the outer to the inner cytosol (for the second instance) could be analysed by the use of a reaction–diffusion model. Again if σ also refers to the fraction of (photo)respired CO_2 molecules that have to experience r_{ch}, in addition to r_{wp} and r_{sc}, if they are to escape from being refixed, Eqs. (13–15) also apply to these two special cases.

Results and discussion

Dependence of A and $g_{m,app}$ on ω and σ values

Equations for all illustrations in this section are all given in Appendix A. Figure 2 shows the initial section of simulated A–C_i curves for various combinations of ω and σ values, indicating that a change in σ (i.e. the arrangement of chloroplasts and mitochondria in mesophyll cells) had a same magnitude of the effect as a change in ω (i.e. the physical resistance of chloroplast components relative to the total mesophyll resistance). Increasing σ (Fig. 2a) or decreasing ω (Fig. 2b) increased A for a given $g_{m,dif}$. This is largely caused by varying amounts of refixation of (photo)respired CO_2, which become increasingly important with decreasing C_i. For example, the estimated f_{refix} (Eq. 15) was 0.385, 0.333 and 0.285 for the three cases corresponding to solid, long-dashed and short-dashed lines of Fig. 2a, respectively (where r_{sc} was set to have the same value as $1/g_{m,dif}$, and r_{cx} was calculated as $(C_c + x_2)/x_1$, also see Eq. B2 in Tholen et al. 2012). f_{refix} can also be calculated for the three cases of Fig. 2b. Such

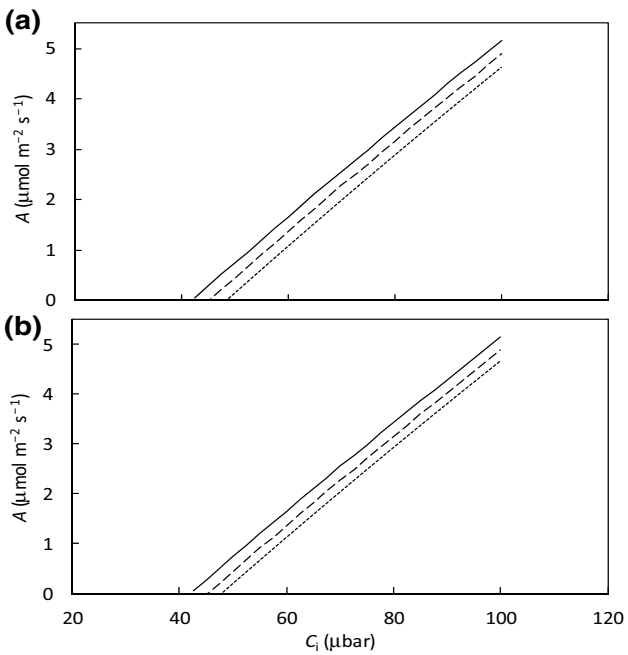

Fig. 2 Simulated net CO_2 assimilation rate (A) as a function of low C_i, under ambient O_2 condition: **a** for three values of σ (*solid line* for $\sigma=1$, *long-dashed line* for $\sigma=0.5$ and *short*-dashed *line* for $\sigma=0$) if parameter ω stays constant at 0.5, and **b** for three values of ω (*solid line* for $\omega=0$, *long*-dashed *line* for $\omega=0.5$ and *short*-dashed *line* for $\omega=0.9$) if parameter σ stays constant at 0.5. Other parameter values used for this simulation: $g_{m,dif}$ = 0.4 mol m^{-2} s^{-1} bar $^{-1}$; V_{cmax} = 80 μmol m^{-2} s^{-1}; K_{mC} = 291 μbar; K_{mO} = 194 mbar; R_d = 1 μmol m^{-2} s^{-1} and Rubisco specificity $S_{c/o}$ = 3.1 mbar μbar^{-1} (the equivalent Γ_* = 34 μbar for the ambient O_2 condition). Simulation used Eqn (18) in Appendix A

differences in f_{refix} can produce a significant difference in A (when C_i is low) and in CO_2 compensation point Γ (Fig. 2). Differences in Γ was already shown by von Caemmerer (2013) between two special cases, i.e. Case I (Fig. 1a) versus Case II (Fig. 1b). With increasing C_i, refixation becomes less important, and differences in A are increasingly negligible (results not shown).

$g_{m,app}$, calculated from Eq. (14), decreased with decreasing C_i, although $g_{m,dif}$ was fixed as constant (Fig. 3). This variation did not occur only if $\sigma = 1$ (the horizontal line in Fig. 3a) or $\omega = 0$ (the horizontal line in Fig. 3b), suggesting the classical g_m model can arise either from $\sigma = 1$ (all mitochondria stay closely behind chloroplasts as if carboxylation and (photo)respiratory CO_2 release occur in one compartment) or from $\omega = 0$ (the chloroplast component in total mesophyll resistance is negligible). The short-dashed line in Fig. 3a represents the case when $\sigma = 0$, corresponding to the original model of Tholen et al. (2012) that applies to the case where all mitochondria locate in the outer cytosol. A change in organelle arrangement within a mesophyll cell resulted in a change in sensitivity of $g_{m,app}$ to C_i as shown by the long-dashed line in Fig. 3a, which lies between the horizontal line and the short-dashed line.

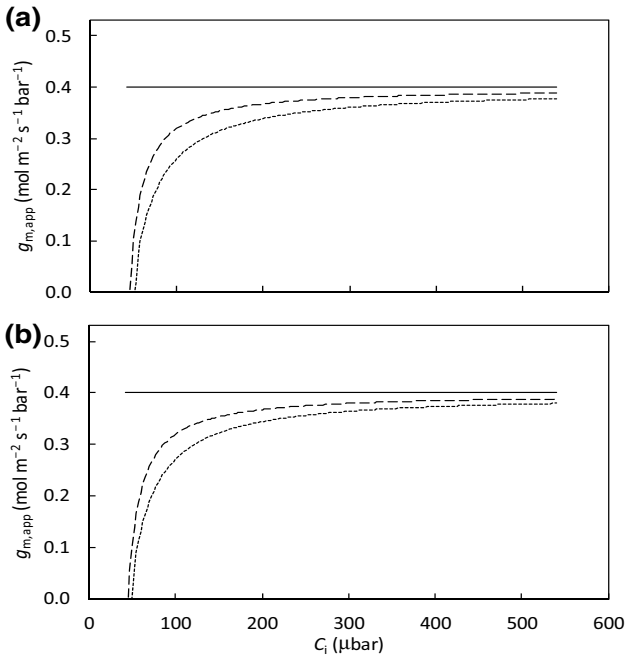

Fig. 3 Simulated apparent mesophyll conductance ($g_{m,app}$) as a function of C_i, under ambient O_2 condition: **a** for three values of σ (*solid line* for $\sigma = 1$, *long-dashed line* for $\sigma = 0.5$ and *short dash line* for $\sigma = 0$) if parameter ω stays constant at 0.5 and **b** for three values of ω (*solid line* for $\omega = 0$, *long-dashed line* for $\omega = 0.5$ and *short-dashed line* for $\omega = 0.9$) if parameter σ stays constant at 0.5. The value of J used for simulation was 125 µmol m^{-2} s^{-1}. Other parameter values as in Fig. 2. Simulation used the method as described in Appendix A

The model of Tholen et al. (2012) as special case of the generalised model

It is evident from our analysis above that the original model of Tholen et al. (2012) applies to a special case of our generalised model, where (photo)respired CO_2 is entirely released in the outer cytosol between the plasmalemma and the chloroplast layer. However, this case can hardly be observed in real leaves, where mitochondria occur mostly in the cell interior, closely behind chloroplasts (Sage and Sage 2009; Hatakeyama and Ueno 2016).

In our model, as stated earlier for the purpose of retaining model simplicity, a large part of $r_{cytosol}$ is lumped into r_{wp}, and the remaining part is lumped into r_{ch}. For their model, Tholen et al. (2012) assumed that cytosolic resistance is negligible. Although this assumption was made, as described by Tholen et al. (2012), only for the purpose of simplicity, it has implications. If $r_{cytosol}$ is so small that it can be neglected, then CO_2 diffusion is so fast that the CO_2 concentration anywhere in the cytosol should be the same independent of where the mitochondria are located, provided the cytosol is continuous (for example, allowed by an S_c/S_m lower than 1). Then the position of the mitochondria does not have any effect on f_{refix}. Practically, the four cases for scenarios (a), (d), (e) and (f) in Fig. 1 would all be equivalent to the original Tholen et al. model ($\sigma = 0$). This is because $\lambda = 0$ in the case of Fig. 1a, or $k = 0$ in cases of Fig. 1d,e, or both λ and $k = 0$ in the case of Fig. 1 f. In this context, the original model of Tholen et al. (2012) would become an alternative special case of our model, that is, assuming that CO_2 in the cytosol is completely mixed. If $r_{cytosol}$ is indeed negligible, then cases in Fig. 1d,e,f are no longer needed for developing the generalised model.

Can parameters ω and σ in the generalised model be measured?

In real cells, $r_{cytosol}$ may be very high (Peguero-Pina et al. 2012; Berghuijs et al. 2015) and therefore cannot be neglected. Then, $r_{cytosol}$ should appear in the model, making it dependent on the detailed morphology of the cell and location of mitochondria and chloroplasts, and this would require the use of a reaction–diffusion model. Within the resistance model framework, Tholen et al. (2012, in their Appendix C) and Tomas et al. (2013) analysed the possible effects of $r_{cytosol}$ in relation to S_c/S_m on g_m. In our generalised model, any significant $r_{cytosol}$ value would mainly be lumped into parameter ω, while parameter σ encompasses any combination of chloroplast–mitochondria arrangement and S_c/S_m. This means that parameters ω and σ in our model can be experimentally measured, at least approximately.

Individual physical resistance components r_{wall}, $r_{plasmalemma}$, $r_{cytosol}$, $r_{envelope}$ and r_{stroma} have been calculated

from microscopic measurements on leaf anatomy (Peguero-Pina et al. 2012; Tosens et al. 2012a, b; Tomas et al. 2013; Berghuijs et al. 2015), despite the uncertainties in the value of gas diffusion coefficients used for the calculation. These measurements can provide basic data to derive ω. For example, Berghuijs et al. (2015) showed that for tomato leaves, ω was about 0.65. Parameter σ depends on both S_c/S_m and the relative position of mitochondria to chloroplasts. In most annuals especially when leaves are young, S_c/S_m is high (close to 1; Sage and Sage 2009; Terashima et al. 2011; Berghuijs et al. 2015), σ should be predominantly determined by the relative position of mitochondria (i.e. $\sigma \approx \lambda$, the proportion of mitochondria lying in the inner cytosol). Hatakeyama and Ueno (2016) showed that for 10 C_3 grasses most mitochondria are located on the vacuole side of chloroplast in mesophyll cells and their data suggested that λ varies from 0.61 to 0.92 among these species, with an average of 0.8. Assuming these values are representative for young leaves of annual C_3 species, then the collective value of $\omega(1-\sigma)$ in our model is about 0.13, a value closer to what the classical model represents (0) than the model of Tholen et al. (2012) does.

However, in woody species (e.g. Tosens et al. 2012a) or in old leaves of annual species (Busch et al. 2013), S_c/S_m can be as low as 0.4. Because the chloroplast coverage is low, especially when combined with a low $r_{cytosol}$ (Tosens et al. 2012b), $\omega(1-\sigma)$ must be close to what the model of Tholen et al. (2012) represents. However, parameter σ is hard to determine directly for this case as its component k may be interdependent on its other component λ. In such a case, σ may only be a "fudge factor" that lumps λ and S_c/S_m in a complicated manner, which may be elucidated by using reaction–diffusion models. Alternatively, the collective value of $\omega(1-\sigma)$ could be estimated (together with $g_{m,dif}$) by fitting Eq. (18) in AppendixA to gas exchange data at various O_2 levels, and then σ could be calculated if anatomical measurements reliably estimate ω; but this approach needs to be tested.

Can two-resistance models exclusively explain observed variable $g_{m,app}$?

Compared with the classical model that uses a single resistance parameter, both Tholen et al. (2012) model and our generalised model partition mesophyll resistance into two components. In Fig. 3, we have shown the dependence in the sensitivity of $g_{m,app}$ on both ω and σ values. Our illustration for the general case (Fig. 3) still agrees qualitatively with Tholen et al. (2012), who, based on their two-resistance model, clearly showed the sensitivity of $g_{m,app}$ to the ratio of $(F+R_d)$ to A. They suggested that this sensitivity could explain the commonly observed decrease of $g_{m,app}$ with decreasing C_i with a low C_i range (e.g. Flexas et al. 2007; Yin et al. 2009). Since the $(F+R_d)/A$ ratio also varies with irradiance and temperature, one might wonder if their model explains any variation of $g_{m,app}$ with these factors. However, their framework, as stated by Tholen et al. (2012), cannot explain the commonly observed responses of $g_{m,app}$ to a change in C_i within the higher C_i range (e.g. Flexas et al. 2007) or in I_{inc} (e.g. Yin et al. 2009; Douthe et al. 2012) or in temperature (e.g. Bernacchi et al. 2002; Yamori et al. 2006; Evans and von Caemmerer 2013; von Caemmerer and Evans 2015). In fact, Gu and Sun (2014) showed that even the response of $g_{m,app}$ to a change in C_i (including the low C_i range) could be simply due to possible errors in measuring A, J and C_i, or to possible errors in estimating R_d and $S_{c/o}$, or could be due to the use of the NADPH-limited form of the FvCB model by the variable J method when the true form is the ATP-limited equation.

In the absence of any measurement errors, can the sensitivity of $g_{m,app}$ to the $(F+R_d)/A$ ratio be considered as the only explanation of $g_{m,app}$ sensitivity to C_i within the low C_i range? Here we want to (re-)state that the decline of $g_{m,app}$ with decreasing C_i below a certain level, as assessed by the variable J method of Harley et al. (1992), can also be accounted for by the fact that the method is based only on the A_j equation of the FvCB model (Yin et al. 2009). When C_i is decreasing towards the CO_2 compensation point, A is increasingly limited by A_c rather than by A_j. Under such conditions, part of the e^- fluxes may become alternative e^- transport not used in support of CO_2 fixation and photorespiration. So, use of the variable J method, which is based on Eq. (1) and the A_j equation of the FvCB model, may lead to underestimation of $g_{m,app}$. This is shown in Fig. 4a, in which for a given fixed $g_{m,dif}$ (0.4 mol m^{-2} s^{-1} bar $^{-1}$), $g_{m,app}$ decreased with decreasing C_i as expected from Eq. (14); but $g_{m,app}$ decreased more sharply if A_j part of the model was applied to the low C_i range which was actually A_c-limited. One would expect that $g_{m,dif}$ calculated back from using the simulated A should be equal to the pre-fixed $g_{m,dif}$ (0.4 mol m^{-2} s^{-1} bar $^{-1}$). However, the calculated $g_{m,dif}$ if using only the A_j part of the model as in the variable J method gave artifactually lower $g_{m,dif}$ values for the A_c-limited part (Fig. 4b). In this calculation shown in Fig. 4, J was assumed to be a constant across C_i levels, whereas actual fluorescence measured J may decline slightly with lowering C_i in the low C_i range (e.g. Cheng et al. 2001), probably reflecting a feedback effect of Rubisco limitation on electron transport. However, the feedback is not so complete that the variable J method, if applied to the low C_i range, always tends to underestimate the actual mesophyll conductance. For these reasons, Yin and Struik (2009) stated that the proposal of the variable J method to be applied to the lower range of A–C_i curve where J is variable (Harley et al. 1992) is inappropriate. A good correlation between values of g_m estimated from the

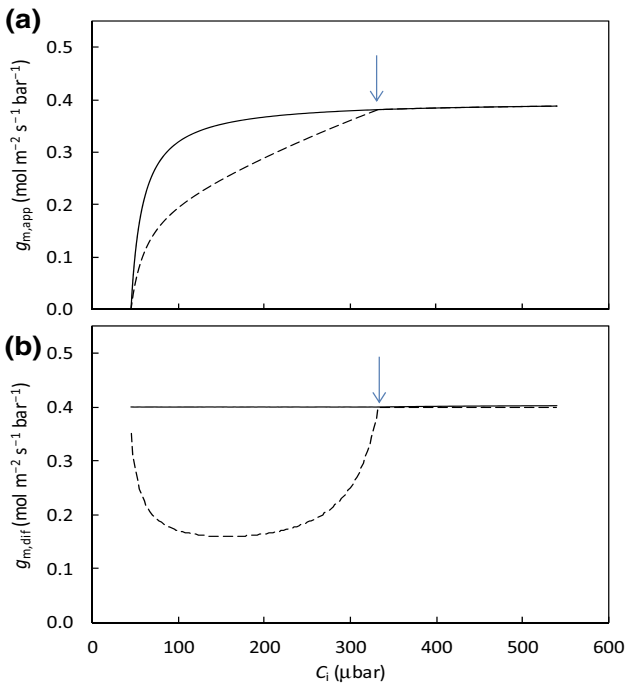

Fig. 4 Simulated apparent mesophyll conductance $g_{m,app}$ (**a**) or intrinsic diffusional mesophyll conductance $g_{m,dif}$ (**b**) as a function of C_i under ambient O_2 condition, with $\sigma=0.5$ and $\omega=0.5$. $g_{m,app}$ and $g_{m,dif}$ were calculated using C_c derived either from the full FvCB model (*solid lines*) or from the A_j part of the model as in the variable J method (dashed *lines*). The *arrow* indicates the transition point from being A_c-limited to being A_j-limited. Input parameter values used for simulation are given in Figs. 2 and 3. Simulation used the method as described in Appendix A

variable J method and the online isotopic method but not when C_i is <200 µmol mol^{-1} (Vrábl et al. 2009) further supports our statement.

Conclusions

The model of Tholen et al. (2012) considers the partitioning of intrinsic diffusion resistance but with little explicit consideration of intracellular organelle arrangements, especially not intracellular position of mitochondria and chloroplasts. We introduced the parameter σ for defining the fraction of (photo) respired CO_2 molecules that have to experience all r_{ch}, in addition to r_{wp} and r_{sc}, if these CO_2 molecules are to escape from being refixed. σ has a value between 0 and 1, depending on the arrangement of organelles within mesophyll cells, i.e. (1) the relative position of chloroplasts and mitochondria and (2) the size of the gaps between chloroplasts. This provides a simple generalised form of the Tholen et al. model in a way that the latter model, Eq. (4), is still valid for all organelle arrangement scenarios if ω is replaced by $\omega(1-\sigma)$. The two parameters of our generalised model can be amenable to experimental estimation for young leaves of annual species where chloroplast coverage continues along the mesophyll cell periphery ($S_c/S_m = 1$). The model of Tholen et al. (2012) is the special case of our model when $\sigma = 0$, which arises either from $\lambda=0$ (no mitochondria in the inner cytosol) combined with $S_c/S_m = 1$ or from a negligible $r_{cytosol}$ combined with $S_c/S_m < 1$. Our model shows that the sensitivity of $g_{m,app}$ to $(F+R_d)/A$ lies somewhere in between the classical method ($\omega = 0$ or $\sigma = 1$, non-sensitive) and the Tholen et al. model ($\sigma = 0$, highly sensitive). Therefore, Tholen et al. (2012) may have overstated that the sensitivity of $g_{m,app}$ on $(F+R_d)/A$ in their model explains the commonly reported decline of $g_{m,app}$ with decreasing C_i in the low C_i range. In fact, the decline, if not due to measurement or parameter–estimation errors, could also be attributed, at least partly, to the variable J method that is wrongly applied to low C_i range where CO_2 assimilation is actually limited by Rubisco activity.

Acknowledgements This research is financed in part by the Bio-Solar Cells open innovation consortium, supported by the Dutch Ministry of Economic Affairs, Agriculture and Innovation. We thank the reviewers and the coordinating editor (Dr. A.B. Cousins) for their very useful comments on the previous versions of the manuscript.

Appendix A

Equations used for simulation in this paper

The FvCB model calculates carboxylation rate (V_c) as $C_c x_1/(C_c+x_2)$, and photorespiratory CO_2 release F as $(\Gamma_*/C_c)V_c$; so, F can be expressed as follows:

$$F = \frac{\Gamma_* x_1}{C_c + x_2} \tag{16}$$

where Γ_* is the CO_2 compensation point in the absence of R_d (Γ_* depends on O_2 partial pressure O and Rubisco specificity $S_{c/o}$ as $0.5O/S_{c/o}$), $x_1=J/4$ and $x_2=2\Gamma_*$ for the A_j-limited conditions and $x_1=V_{cmax}$ (maximum carboxylation activity of Rubisco) and $x_2=K_{mC}(1+O/K_{mO})$ for the A_c-limited conditions (K_{mC} and K_{mO} are Michaelis–Menten constants of Rubisco for CO_2 and O_2, respectively).

Also C_c can be solved from the FvCB model as

$$C_c = \frac{\Gamma_* x_1 + x_2(A + R_d)}{x_1 - (A + R_d)} \tag{17}$$

Combining Eqs. (16–17) with Eq. (13) and solving the combined equations for A, step by step, result in a quadratic solution:

$$A = (-b - \sqrt{b^2 - 4ac})/(2a) \tag{18}$$

where $a = x_2 + \Gamma_*[1 - \omega(1 - \sigma)]$

$$b = \omega(1 - \sigma)\left(R_d x_2 + \Gamma_* x_1\right) - \left\{x_2 + \Gamma_*[1 - \omega(1 - \sigma)]\right\} \left(x_1 - R_d\right) - g_{m,dif}\left(C_i + x_2\right)\left(x_2 + \Gamma_*\right)$$

$$c = -\omega(1 - \sigma)\left(R_d x_2 + \Gamma_* x_1\right)\left(x_1 - R_d\right) + g_{m,dif}\left(x_2 + \Gamma_*\right) [x_1\left(C_i - \Gamma_*\right) - R_d\left(C_i + x_2\right)]$$

Equation (18) was used to generate A–C_i response curves as shown in Fig. 2 for a given set of input parameter values.

When A is solved, C_c can be solved from Eq. (18), and the solved C_c was used as input to Eq. (1) to calculate $g_{m,app}$. Alternatively, $g_{m,app}$ can be calculated directly from Eq. (14) with F calculated from eqn (16). This gave $g_{m,app}$ as shown in Figs. 3 and 4a.

When A, C_c and F are all known, one can calculate back for $g_{m,dif}$:

$$g_{m,dif} = \frac{A + \omega(1 - \sigma)(F + R_d)}{C_i - C_c} \tag{19}$$

When C_c and F are both based on the A_j-limited part of the FvCB model, then eqn (19) gives an equation that calculates $g_{m,diff}$, like the variable J method of Harley et al. (1992) for calculating $g_{m,app}$. This was used to generate Fig. 4b.

References

Berghuijs HNC, Yin X, Ho QT, van der Putten PEL, Verboven P, Retta MA, Nicolaï BM, Struik PC (2015) Modeling the relationship between CO_2 assimilation and leaf anatomical properties in tomato leaves. Plant Sci 238:297–311

Berghuijs HNC, Yin X, Ho QT, Driever SM, Retta MA, Nicolaï BM, Struik PC (2016) Mesophyll conductance and reaction-diffusion models for CO_2 transport in C_3 leaves; needs, opportunities and challenges. Plant Sci 252:62–75

Bernacchi CJ, Portis AR, Nakano H, von Caemmerer S, Long SP (2002) Temperature response of mesophyll conductance. Implication for the determination of Rubisco enzyme kinetics and for limitations to photosynthesis *in vivo*. Plant Physiol 130:1992–1998

Busch FA, Sage TL, Cousins AB, Sage RF (2013) C_3 plants enhance rates of photosynthesis by reassimilating photorespired and respired CO_2. Plant Cell Environ 36:200–212

Cheng L, Fuchigami LH, Breen PJ (2001) The relationship between photosystem II efficiency and quantum yield for CO_2 assimilation is not affected by nitrogen content in apple leaves. J Exp Bot 52:1865–1872

Douthe C, Dreyer E, Brendel O, Warren CR (2012) Is mesophyll conductance to CO_2 in leaves of three *Eucalyptus* species sensitive to short-term changes of irradiance under ambient as well as low O_2? Funct Plant Biol 39:435–448

Evans JR, von Caemmerer S (2013) Temperature response of carbon isotope discrimination and mesophyll conductance in tobacco. Plant Cell Environ 36:745–756

Evans JR, Sharkey TD, Berry JA, Farquhar GD (1986) Carbon isotope discrimination measured concurrently with gas exchange to investigate CO_2 diffusion in leaves of higher plants. Aust J Plant Physiol 13:281–292

Evans JR, Kaldenhoff R, Genty B, Terashima I (2009) Resistances along the CO_2 diffusion pathway inside leaves. J Exp Bot 60:2235–2248

Farquhar GD, von Caemmerer S, Berry JA (1980) A biochemical model of photosynthetic CO_2 assimilation in leaves of C_3 species. Planta 149:78–90

Flexas J, Diaz-Espejo A, Galmes J, Kaldenhoff R, Medrano H, Ribas-Carbó M (2007) Rapid variation of mesophyll conductance in response to changes in CO_2 concentration around leaves. Plant Cell Environ 30:1284–1298

Gu L, Sun Y (2014) Artefactual responses of mesophyll conductance to CO_2 and irradiance estimated with the variable J and online isotope discrimination methods. Plant Cell Environ 37:1231–1249

Harley PC, Loreto F, Di Marco G, Sharkey TD (1992) Theoretical considerations when estimating the mesophyll conductance to CO_2 flux by analysis of the response of photosynthesis to CO_2. Plant Physiol 98:1429–1436

Hatakeyama Y, Ueno O (2016) Intracellular position of mitochondria and chloroplasts in bundle sheath and mesophyll cells of C_3 grasses in relation to photorespiratory CO_2 loss. Plant Prod Sci 19:540–551

Kebeish R, Niessen M, Thirshnaveni K, Bari R, Hirsch H-J, Rosenkranz R, Stäbler N, Schönfeld B, Kreuzaler F, Peterhänsel C (2007) Chloroplastic photorespiratory bypass increases photosynthesis and biomass production in *Arabidopsis thaliana*. Nature Biotechnol 25:593–599

Peguero-Pina JJ, Flexas J, Galmes J, Niinemets Ü, Sancho-Knapik D, Barredo G, Villarroya D, Gil-Pelegrin E (2012) Leaf anatomical properties in relation to differences in mesophyll conductance to CO_2 and photosynthesis in two related Mediterranean *Abies* species. Plant Cell Environ 35:2121–2129

Pons TL, Flexas J, von Caemmerer S, Evans JR, Genty B, Ribas-Carbo M, Brugnoli E (2009) Estimating mesophyll conductance to CO_2: methodology, potential errors, and recommendations. J Exp Bot 60:2217–2234

Sage TL, Sage RF (2009) The functional anatomy of rice leaves: implications for refixation of photorespiratory CO_2 and effects to engineer C_4 photosynthesis into rice. Plant Cell Physiol 50:756–772

Tazoe Y, von Caemmerer S, Badger MR, Evans JR (2009) Light and CO_2 do not affect the mesophyll conductance to CO_2 diffusion in wheat leaves. J Exp Bot 60:2291–2301

Tcherkez G, Boex-Fontvieille E, Mahe A, Hodges M (2012) Respiratory carbon fluxes in leaves. Curr Opin Plant Biol 15:308–314

Terashima I, Hanba YT, Tholen D, Niinemets Ü (2011) Leaf functional anatomy in relation to photosynthesis. Plant Physiol 155:108–116

Tholen D, Zhu X-G (2011) The mechanistic basis of internal conductance: a theoretical analysis of mesophyll cell photosynthesis and CO_2 diffusion. Plant Physiol 156:90–105

Tholen D, Ethier G, Genty B, Pepin S, Zhu X-G (2012) Variable mesophyll conductance revisited: theoretical background and experimental implications. Plant Cell Environ 35:2087–2103

Tomas M, Flexas J, Copolovici L, Galmes J, Hallik L, Medrano H, Ribas-Carbo M, Tosens T, Vislap V, Niinemets Ü (2013) Importance of leaf anatomy in determining mesophyll diffusion conductance to CO_2 across species: quantitative limitations and scaling up by models. J Exp Bot 64:2269–2281

Tosens T, Niinemets Ü, Vislap V, Eichelmann H, Castro Diez P (2012a) Developmental changes in mesophyll diffusion conductance and photosynthetic capacity under different light and water availabilities in *Populus tremula*: how structure constrains function. Plant Cell Environ 35:839–856

Tosens T, Niinemets Ü, Westoby M, Wright IJ (2012b) Anatomical basis of variation in mesophyll resistance in eastern Australian sclerophylls: news of a long and winding path. J Exp Bot 63:5105–5119

von Caemmerer S (2013) Steady-state models of photosynthesis. Plant Cell Environ 36:1617–1630

von Caemmerer S, Evans JR (1991) Determination of the average partial pressure of CO_2 in chloroplasts from leaves of several C_3 plants. Aust J Plant Physiol 18:287–305

von Caemmerer S, Evans JR (2015) Temperature responses of mesophyll conductance differ greatly between species. Plant Cell Environ 38:629–637

von Caemmerer S, Evans JR, Hudson GS, Andrews TJ (1994) The kinetics of ribulose-1,5-bisphosphate carboxylase/oxygenase in vivo inferred from measurements of photosynthesis in leaves of transgenic tobacco. Planta 195:88–97

Vrábl D, Vašková M, Hronková M, Flexas J, Šantrůček J (2009) Mesophyll conductance to CO_2 transport estimated by two independent methods: effect of variable CO_2 concentration and abscisic acid. J Exp Bot 60:2315–2323

Yamori W, Noguchi K, Hanba YT, Terashima I (2006) Effects of internal conductance on the temperature dependence of the photosynthetic rate in spinach leaves from contrasting growth temperatures. Plant Cell Physiol 47:1069–1080

Yin X, Struik PC (2009) Theoretical reconsiderations when estimating the mesophyll conductance to CO_2 diffusion in leaves of C_3 plants by analysis of combined gas exchange and chlorophyll fluorescence measurements. Plant Cell Environ 32:1513–1524 with corrigendum in 33:1595

Yin X, Struik PC, Romero P, Harbinson J, Evers JB, van der Putten PEL, Vos J (2009) Using combined measurements of gas exchange and chlorophyll fluorescence to estimate parameters of a biochemical C_3 photosynthesis model: a critical appraisal and a new integrated approach applied to leaves in a wheat (*Triticum aestivum*) canopy. Plant Cell Environ 32:448–464